Topological polaritons and excitons in garden-variety systems

Charles-Edouard Bardyn, Torsten Karzig, Gil Refael, and Timothy C. H. Liew

Phys. Rev. B **91**, 161413 — Published 29 April 2015

DOI: 10.1103/PhysRevB.91.161413

Topological Polaritons and Excitons in Garden Variety Systems

Charles-Edouard Bardyn*,[1] Torsten Karzig*,[1] Gil Refael,[1] and Timothy C. H. Liew[2]

[1]*Institute for Quantum Information and Matter, Caltech, Pasadena, California 91125, USA*
[2]*Division of Physics and Applied Physics, Nanyang Technological University 637371, Singapore*

We present a practical scheme for creating topological polaritons in garden variety systems based, for example, on zinc-blende semiconductor quantum wells. Our proposal requires a moderate magnetic field and a potential landscape which can be implemented, e.g., via surface acoustic waves or patterning. We identify indirect excitons in double quantum wells as an appealing alternative for topological states in exciton-based systems. Topological polaritons and indirect excitons open a new frontier for topological states in solid-state systems, which can be directly probed and manipulated while offering a system with nonlinear interactions.

PACS numbers: 71.35.-y,71.36.+c,85.75.-d,42.70.Qs

Topological states and phases in quantum systems have yielded a wealth of exotic phenomena, with measurable signatures at edges and surfaces. In electronic topological insulators, what would otherwise seem a usual semiconductor may exhibit conducting states at its edges [1, 2]. Similar physics has emerged in photonic systems, where theory [3–6] was followed by demonstrations of topological behavior in microwave-range photonic crystals [7] and arrays of coupled optical resonators [8, 9] or waveguides [10]. Photons propagating in chiral edge states are protected from backscattering with material imperfections, and may revolutionize photonic circuitry [11].

However, these developments are by and large due to linear optical effects, while applications in photonic circuitry often require nonlinear optical properties. Hence the importance of the recently proposed "topological polaritons" [12], which combine topology and nonlinear properties via light-matter interactions. Excitons interact with one another and, when placed in an optical microcavity, hybridize into so-called exciton-polaritons which balance a strong exciton nonlinearity with a significant optical component [13, 14]. Polaritons are well-known for their integer spin degree of freedom, which allows for spin currents [15, 16] and a range of optical switches/transistors [17–19]. Spin currents can also be generated using indirect excitons in double quantum wells [20], and the long lifetime of these particles has allowed excitonic transistors [21] with optical coupling and control [22]. Both indirect-exciton and polariton systems are strongly influenced by disorder, which induces scattering and weakens signals carried by ballistic particle propagation. Topology promises to remedy this issue, as was envisioned several years ago for excitons at the surface of 3D topological insulators [23] or in coupled quantum wells close to ferromagnetic insulating films [24], and more recently for exciton condensates in bilayer HgTe [25] and InAs/GaSb [26] quantum wells.

In this Letter, we demonstrate theoretically that topological excitonic states can be realized using surprisingly simple ingredients present in two very common types of systems: (i) polaritons in semiconductor microcavities, and (ii) indirect excitons in coupled quantum wells. In scenario (i), polaritons exhibit two spin states coupled by the transverse-electric-transverse-magnetic (TE-TM) splitting [27] arising from the polarization-dependent reflectivity of the cavity mirrors, supplemented by a weaker but complementary polarization splitting of (direct) excitons stemming from the long-range exchange interaction between electrons and holes [28]. In scenario (ii), we consider a pair of coupled quantum wells in close enough proximity for long-lived indirect excitons to form from electrons and holes in different layers. Four different spin states (including bright and dark exciton spin states) experience a Dresselhaus-type spin-orbit coupling [29].

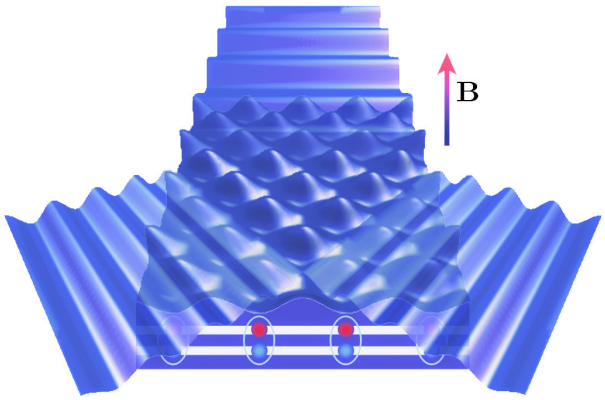

FIG. 1: (Color online) Schematic view of a typical system supporting topological polaritons or indirect excitons: Surface acoustic waves modulate the thickness of quantum wells and interfere to generate a triangular lattice potential for particles in the plane. Whether multiple quantum wells are coupled together, as in the depicted system of indirect excitons, or are strongly mixed with light inside a microcavity, combining the periodic potential with an applied Zeeman field **B** leads to topologically non-trivial bands.

In both scenarios, we start from topologically trivial ingredients and use a magnetic field to break time-reversal symmetry. The natural sensitivity of excitons to applied magnetic fields circumvents the need for materials with large gyrotopic permeability, while enabling operation at

optical frequencies. A periodic exciton or polariton potential is also required to open a global (topological) gap, as discussed in Ref. [12]. Such potential modulations can be implemented by applying surface acoustic waves [30–33] (see Fig. 1) or engineering permanent lattices [34, 35].

The simplification at the root of this paper stems from the linear-to-circular polarization conversion naturally present in garden variety systems of indirect excitons and polaritons [15, 20, 36]. Topological polaritons can be created by a "winding coupling" of topologically trivial exciton and photon bands [12]. While the original proposal of Ref. [12] exploited the pseudo-spin-orbit coupling present in the underlying *electronic* system to realize such a winding, here we take advantage of the built-in splitting of TE and TM *photonic* modes in typical planar microcavities [27]. In a basis of right- and left-handed circularly polarized modes $(\phi_+(\mathbf{k}), \phi_-(\mathbf{k}))$, this TE-TM polarization splitting can be described by the Hamiltonian [15, 16]

$$\mathcal{H}_\phi^{\mathrm{TE-TM}} = \Delta_\phi(k) \begin{pmatrix} 0 & e^{-2i\varphi(\mathbf{k})} \\ e^{2i\varphi(\mathbf{k})} & 0 \end{pmatrix}. \qquad (1)$$

In this basis, the coupling between modes with opposite circular polarizations (or spin projections along the z-direction) exhibits a double winding in terms of the polar angle $\varphi(\mathbf{k})$ associated with $\mathbf{k}$. Physically, this can be understood from the fact that coupling the mode $\phi_\mp(\mathbf{k})$ to $\phi_\pm(\mathbf{k})$ requires a change of ± 2 of total angular momentum in the z-direction [37].

When coupled to excitonic modes (χ_+, χ_-) (where $\pm$ distinguishes spin projections along z as above, and explicit $\mathbf{k}$-dependences are omitted), the photonic modes (ϕ_+, ϕ_-) hybridize into (four) polaritonic modes [38]. Here we assume that the exciton-photon coupling is much larger than the polarization splitting between photonic (or excitonic) modes, which is typically satisfied for polaritons in microcavities [36]. This allows us to focus on the lower polariton branch consisting of two modes of the form $\psi_\pm = P_0\phi_\pm + X_0\chi_\pm + X_{\pm 2}\chi_\mp$, where P_0, X_0 and $X_{\pm 2}$ are complex (Hopfield) coefficients determined by the nature of the exciton-photon coupling, with indices indicating the change of total angular momentum required for each coupling (for angular momentum conservation, $X_{\pm 2}$ must be of the form $e^{\pm 2i\varphi}$ and vanish at $\mathbf{k} = \mathbf{0}$ to avoid any singularity, while P_0 and X_0 cannot contain any winding). Instead of taking advantage, as in Ref. [12], of the relatively large coupling $X_{\pm 2}$ that can appear at large momenta, here we consider the typical regime where, at finite but low momenta, $X_{\pm 2} \approx 0$ and polarization splitting dominates. In this low-momentum regime more accessible to experiments [14], the polaritonic modes (ψ_+, ψ_-) directly inherit the winding coupling originating from Eq. (1). More explicitly, one finds

$$\mathcal{H}_\psi^{\mathrm{TE-TM}} \begin{pmatrix} \psi_+ \\ \psi_- \end{pmatrix} = \Delta_\psi \begin{pmatrix} 0 & e^{-2i\varphi} \\ e^{2i\varphi} & 0 \end{pmatrix} \begin{pmatrix} \psi_+ \\ \psi_- \end{pmatrix}, \qquad (2)$$

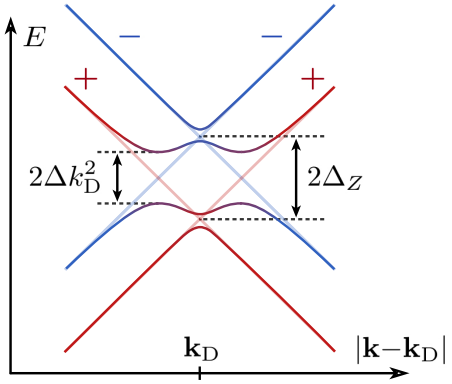

FIG. 2: Opening up a topological gap: Cross-sectional view of the typical polariton band structure found at a Dirac point (located at $\mathbf{k}_{\mathrm{D}}$) generated using a periodic (e.g., triangular lattice) potential. A finite Zeeman field splits the bands corresponding to + and − circular polarizations into two Dirac cones (shown in faint red and blue) by $2\Delta_Z$, leading to a well-defined ring of resonance. The TE-TM (winding) coupling (2) of strength $\Delta k_{\mathbf{D}}^2$ then opens a topological gap, resulting in hybridized bands (solid lines) with Chern number ± 2.

with coupling strength

$$\Delta_\psi = |P_0|^2\Delta_\phi + |X_0|^2\Delta_\chi, \qquad (3)$$

where $\Delta_\chi \equiv \Delta_\chi(k)$ denotes the (much weaker) splitting of excitonic modes due to electron-hole exchange interaction [28]. The form and amplitude of Δ_ψ strongly depends on the exciton-photon detuning, which we assume to be much smaller than the exciton-photon coupling strength. For small $k \equiv |\mathbf{k}|$, $\Delta_\psi(k) \approx \Delta k^2$ [27, 36]. The winding coupling (Eq. (2)) is readily accessible in experiments, giving rise to the optical spin Hall effect [15, 16] and spin-to-angular momentum conversion [37].

Topological states emerge very naturally when combining the (double) winding coupling of Eq. (2) with another type of polarization splitting: the one induced by a magnetic field, which provides the time-reversal symmetry breaking crucially required for the appearance of unidirectional (chiral) edge states (as we demonstrate below). Magnetic fields act on polaritons via the magnetic moment of their excitonic component. When applied in the z-direction, a field of strength B shifts polaritonic modes $\psi_\pm$ in energy by $\pm\Delta_Z = \pm\frac{1}{2}|X_0|(g_e - g_h)\mu_B B$, where g_e and g_h are the electron and hole g-factors, and μ_B is the Bohr magneton. To understand how topology arises in this scenario, it is instructive to examine what happens at a single crossing (or "Dirac point") between polarization-degenerate polariton bands. As depicted in Fig. 2, bands with opposite polarizations (+ and −) split by $2\Delta_Z$ when introducing a magnetic field. Due to the TE-TM splitting of Eq. (2), a *topological* gap then opens along the resulting ring of resonance. Intuitively, the topological nature of this gap can be understood by noticing that the hybridized bands consist of eigenstates which, described

as spinors on the Bloch sphere, *fully* wrap around the sphere as $\mathbf{k}$ runs over all momenta: while increasing $|\mathbf{k}|$ through the resonance flips the spinor from ψ_+ to ψ_- (or vice versa), the winding coupling $e^{-2i\varphi(\mathbf{k})}$ leads to an azimuthal twist which completes the (double) wrapping of the unit sphere. In practice, the isolated band crossing (or Dirac point) required for the above topological behavior can be obtained by introducing a periodic potential for polaritons (i.e., for excitons or/and photons) [39]. Triangular or hexagonal lattice potentials — exhibiting Dirac points — are particularly suitable for this purpose, although other geometries can also be considered [40].

To demonstrate that our scheme leads to the emergence of topological states, we now examine a system with edges and derive the exact form of its spectrum by a plane-wave expansion approach (instead of a less precise tight-binding approximation). We consider a ribbon-type geometry where the system is periodic in the x-direction and finite in the y-direction (with Dirichlet boundary conditions), and experiences a potential

$$V(\mathbf{r}) = V_0 \left[\cos\left(\mathbf{K}_1 \cdot \mathbf{r}\right) + \cos\left(\mathbf{K}_2 \cdot \mathbf{r}\right) + \cos\left(\mathbf{K}_3 \cdot \mathbf{r}\right)\right], \tag{4}$$

with $\mathbf{K}_1 = 4\pi\left(0, 1/\sqrt{3}\right)/a$, $\mathbf{K}_{2,3} = 2\pi\left(1, \pm 1/\sqrt{3}\right)/a$, amplitude V_0 and lattice constant a, which can be realized, e.g., by interfering surface acoustic waves as depicted in Fig. 1. The time-independent Schödinger equation describing the spinor polariton wavefunction is

$$\left[-\frac{\hbar^2}{2m_{\text{eff}}}\left(\frac{\partial^2}{\partial x^2} + \frac{\partial^2}{\partial y^2}\right) + V(x,y) + \sigma\Delta_Z - \varepsilon\right]\psi_\sigma(x,y) + \Delta\left(-\frac{\partial^2}{\partial x^2} + 2i\sigma\frac{\partial^2}{\partial x \partial y} + \frac{\partial^2}{\partial y^2}\right)\psi_{-\sigma}(x,y) = 0, \tag{5}$$

where m_{eff} is the polariton effective mass, $\sigma = \pm 1$ distinguishes right- and left-handed circular polarizations, ε is an energy eigenvalue, and Δ and $2\Delta_Z$ are the TE-TM and Zeeman splittings defined as above. Translation symmetry in the x-direction makes it convenient to express the solutions of Eq. (5) in Bloch form $\psi_\sigma(x,t) = e^{ik_x x}u_\sigma(x,y)$, with $u_\sigma(x,y)$ periodic in x. The periodicity of $u_\sigma(x,y)$ and $V(x,y)$ allows us to expand them as Fourier sums. Substitution into Eq. (5) then leads to an eigenvalue problem for the spectum $\varepsilon(k_x)$.

Concerning parameters, Zeeman splittings of up to 0.2meV have been measured for polaritons in semiconductor microcavities under a magnetic field of 5T [41], while values of up to 1meV are effectively achievable by optically inducing a large spin imbalance [42]. So far polariton potentials with an amplitude of 0.18meV have been realized using surface acoustic waves [32]. Higher values can however be envisioned, given that amplitudes of up to 2meV have been reported in bare quantum wells [31]. Large amplitudes can also be expected for permanent polariton potentials realized by patterning composite materials [34, 35]. As for the TE-TM splitting, typical values are around $\Delta = 0.05\text{meV}\mu\text{m}^2$ [16, 27].

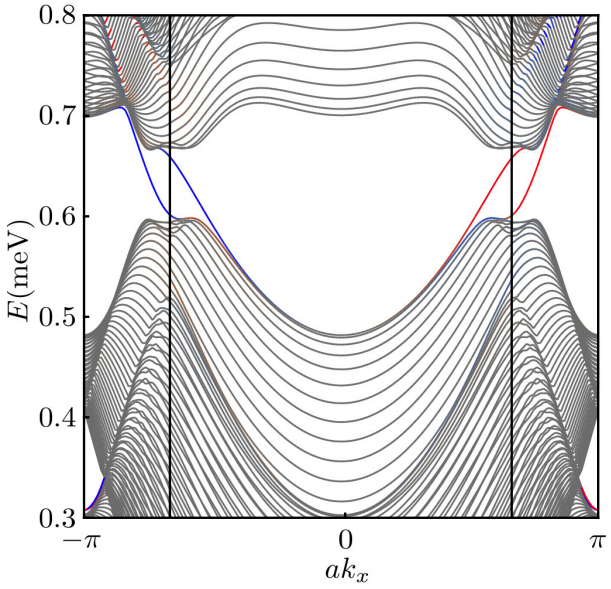

FIG. 3: (Color online) Dispersion of topological polaritons in a triangular lattice (Eq. (4)) with periodic boundary conditions in the x-direction and vanishing (Dirichlet) boundaries conditions in the y-direction. Eigenstates are color-coded according to their proximity to edges — red and blue corresponding to lower and upper edges, respectively — with bulk states shown in grey. Diract points at $ak_x = \pm 2\pi/3$ are shown by vertical lines. Parameters: $\Delta = 0.05\text{meV}\mu\text{m}^2$, $2\Delta_Z = 0.1\text{meV}$, $V_0 = 0.6\text{meV}$, $a = 3\mu\text{m}$, and $m_{\text{eff}} = 7.5 \times 10^{-5} m_0$ [16], where m_0 is the free electron mass.

Fig. 3 illustrates a polariton dispersion obtained using conservative parameters. The topological gap reaches about 0.1meV, which significantly exceeds typical polariton linewidths of the order of tens of μeV [14] (larger gaps can be obtained, e.g., at higher fields). As anticipated above, the gap is bridged by pairs of counter-propagating chiral edge states localized at opposite edges. In accordance with bulk-edge correspondence (see, e.g., Ref. [1]), the lower and upper bands are topologically non-trivial, with Chern numbers $+2$ and -2.

An alternative appealing platform for realizing chiral edge states in exciton-based systems is provided by *indirect excitons*, which are typically formed in structures of coupled quantum wells where electrons and holes are confined in separate wells. Indirect excitons are perhaps best known for their long radiative lifetime resulting from the reduced overlap between electron and hole wavefunctions, which allows for the formation of condensates [44]. They are also appreciated for their four-component spin degree of freedom due to the co-existence of bright excitons (with $J_z = \pm 1$ spin projection normal to the plane) and dark excitons (with $J_z = \pm 2$) at similar energies [29], and for their rich spin dynamics due to spin-orbit interactions [29, 45]. Of particular interest here is the Dresselhaus spin-orbit coupling arising from the intrinsic crystal asymmetry of zinc-blende (e.g., GaAs) crystals, which

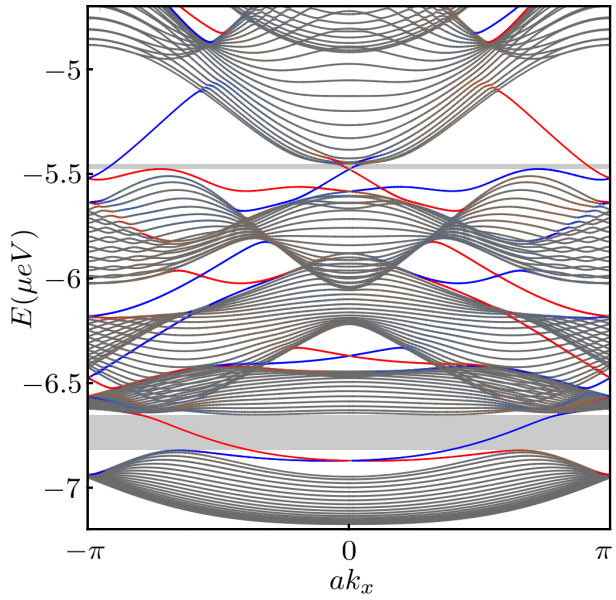

FIG. 4: (Color online) Dispersion of topological indirect excitons obtained from Hamiltonian (6) with a triangular-lattice potential (color-coding as in Fig. 3). Parameters were taken from Ref. [43]: $\beta_e = 2.7\mu\text{eV}\mu\text{m}$, $\beta_h = 0.92\mu\text{eV}\mu\text{m}$, $g_e = 0.01$, $g_h = -8.5 \times 10^{-3}$, $m_e = 0.07m_0$, and $m_h = 0.16m_0$, where m_0 is the free electron mass. A magnetic field $B = 2\text{T}$ was applied with lattice potential $V_0 = 5\mu\text{eV}$ and lattice constant $a = 1.2\mu\text{m}$. In this particular parameter regime, two topological gaps are found in the low-energy spectrum (shaded regions), of 0.17 and $0.03\mu\text{eV}$, respectively.

was similarly invoked in Ref. [24]. In a basis of indirect-exciton spinor wavefunctions $(\psi_{+1}, \psi_{-1}, \psi_{+2}, \psi_{-2})$, the spin dynamics can be captured by the Hamiltonian

$$\mathcal{H} = \begin{pmatrix} \Delta_Z & 0 & \beta_e k_e e^{-i\varphi} & \beta_h k_h e^{-i\varphi} \\ 0 & -\Delta_Z & \beta_h k_h e^{i\varphi} & \beta_e k_e e^{i\varphi} \\ \beta_e k_e e^{i\varphi} & \beta_h k_h e^{-i\varphi} & -\Delta'_Z & 0 \\ \beta_h k_h e^{i\varphi} & \beta_e k_e e^{-i\varphi} & 0 & \Delta'_Z \end{pmatrix}, \quad (6)$$

where β_e and β_h are Dresselhaus constants for electrons and holes, respectively [43]. The wavevectors associated with electrons and holes with effective mass m_e and m_h are related to those of excitons via $\mathbf{k}_e = \frac{m_e}{m_e+m_h}\mathbf{k}$ and $\mathbf{k}_h = \frac{m_h}{m_e+m_h}\mathbf{k}$, respectively. Here the Zeeman splitting differs for bright and dark excitons due to the distinct spin orientations of their electron and hole components: While $\Delta_Z = \frac{1}{2}(g_e - g_h)\mu_B B$ for bright excitons as above, $\Delta'_Z = -\frac{1}{2}(g_e + g_h)\mu_B B$ for dark excitons. Most importantly, the Dresselhaus spin splitting of electron and hole states at non-zero $\mathbf{k}_e$ and $\mathbf{k}_h$ gives rise to coupling terms with single windings $e^{\pm i\varphi}$. Note that we have neglected the Rashba spin-orbit coupling [43, 45], which is only significant in the presence of bulk quantum-well asymmetry or under large electrical bias.

As we demonstrate below, the appearance of winding couplings in a four-component system grants us access to a rich variety of topological features. Similarly as above, topology emerges from the interplay of the winding couplings with a magnetic field, and is only revealed upon introduction of a periodic potential. Below we examine the system with the same ribbon geometry and triangular lattice potential as above (again realizable, e.g., using surface acoustic waves [31]). To derive the spectrum, we use the analog of Eq. (5) with four spin components, an exciton effective mass $m_{\text{ex}} = m_e + m_h$, and spin-orbit coupling and magnetic field described by Eq. (6).

Remarkably, the system allows for multiple bandgaps with different numbers of topologically protected chiral edge states. Bandgaps are either (i) topologically trivial, (ii) topological with a single pair of counter-propagating chiral edge states, or (iii) topological with two such pairs. We present in Fig. 4 the typical indirect-exciton dispersion obtained using experimentally available parameters (taken from Ref. [43]). Two low-energy gaps are shown, exemplifying both cases (ii) and (iii). In practice, parameters can be chosen so as to optimize the size of a particular gap: Under a magnetic field $B = 2\text{T}$ with spin-orbit coupling and indirect-exciton parameters from Ref. [43], the lower energy gap (of type (ii)) can reach about $0.3\mu\text{eV}$ with a periodic potential of amplitude $V_0 = 6\mu\text{eV}$ and lattice constant $a = 1.1\mu\text{m}$, while a gap of type (iii) of about $1.3\mu\text{eV}$ can be obtained by choosing $V_0 = 10\mu\text{eV}$ and $a = 0.75\mu\text{m}$. Note that the maximum achievable gap increases linearly with the applied magnetic field B. Since indirect excitons are typically much longer-lived than polaritons [44], topological gaps of the order of $1\mu\text{eV}$ are in principle well within resolvable range.

In summary, we have demonstrated that topological polaritons and indirect excitons can be realized in garden variety single and double quantum wells made of ordinary materials such as GaAs. Our proposal relies on the TE-TM splitting and Dresselhaus-type spin-orbit coupling naturally present in microcavities or in systems of indirect excitons, respectively. Conservative experimental values for these couplings lead to topological gaps that are larger than the typical polariton/exciton linewidth using readily available magnetic fields (well below 5T) and exciton potential amplitudes (below 1meV). In contrast to the original proposal of Ref. [12], our scheme for topological polaritons does not require excitons and photons to interact resonantly. In fact, a strong photonic component is only required to enhance the typically weak TE-TM splitting of excitons. In more exotic systems with large excitonic TE-TM splitting [46, 47], photons would not be necessary to generate topological states using our scheme. We expect the ability to engineer edge states protected from backscattering to play an important role in the development of a broad variety of exciton-based information processing devices.

During the review process of our manuscript, a related paper appeared in Physical Review Letters [48]. The authors focus on the application of the above generic scheme to create topological polaritons in micropillar arrays de-

scribed by the tight-binding limit of Eq. (5).

This work was funded by the Institute for Quantum Information and Matter, an NSF Physics Frontiers Center with support of the Gordon and Betty Moore Foundation (grant GBMF1250). G. R. acknowledges the Packard Foundation and NSF under DMR-1410435 for their generous support. Financial support from the Swiss National Science Foundation (SNSF) is also acknowledged. T. L. was supported by the Lee Kuan Yew Fellowship.

* These authors contributed equally.

[1] M Z Hasan & C L Kane, Rev. Mod. Phys., **82**, 3045 (2010).
[2] X-L Qi & S-C Zhang, Rev. Mod. Phys., **83**, 1057 (2011).
[3] F D M Haldane & S Raghu, Phys. Rev. Lett., **100**, 013904 (2008).
[4] Z Wang, Y D Chong, J D Joannopoulos, & M Soljačić, Phys. Rev. Lett. **100**, 013905 (2008).
[5] M Hafezi, E A Demler, M D Lukin, & J M Taylor, Nature Phys. **7**, 907 (2011).
[6] K Fang, Z Yu, & S Fan, Nature Photon. **6**, 782 (2012).
[7] Z Wang, Y D Chong, J D Joannopoulos, & M Soljačić, Nature, **461**, 772 (2009).
[8] M Hafezi, S Mittal, J Fan, & J M Taylor, Nature Photon., **7**, 1001 (2013).
[9] N Jia, A Sommer, D Schuster, & J Simon, arXiv: 1309.0878 (2013).
[10] M C Rechtsman, J M Zeuner, Y Plotnik, Y Lumer, D Podolsky, F Dreisow, S Nolte, M Segev, & A Szameit, Nature **496**, 196 (2013).
[11] L Lu, J D Joannopoulos, & M Soljačić, arXiv: 1408.6730 (2014).
[12] T Karzig, C-E Bardyn, N H Lindner, & G Refael, arXiv: 1406.4156 (2014).
[13] A V Kavokin, J J Baumberg, G Malpuech, & F P Laussy, *Microcavities*, Oxford University Press, New York (2007).
[14] I Carusotto & C Cuiti, Rev. Mod. Phys., **85**, 299 (2013).
[15] C Leyder, M Romanelli, J Ph Karr, E Giacobino, T C H Liew, M M Glazov, A V Kavokin, G Malpuech, & A Bramati, Nature Phys., **3**, 628 (2007).
[16] E Kammann, T C H Liew, H Ohadi, P Cilibrizzi, P Tsotsis, Z Hatzopoulos, P G Savvidis, A V Kavokin, & P G Lagoudakis, Phys. Rev. Lett., **109**, 036404 (2012).
[17] C Adrados, T C H Liew, A Amo, M D Martin, D Sanvitto, C Antón, E Giacobino, A Kavokin, A Bramati, & L Viña, Phys. Rev. Lett., **107**, 146402 (2011).
[18] M De Giorgi, D Ballarini, E Cancellieri, F M Marchetti, M H Szymanska, C Tejedor, R Cingolani, E Giacobino, A Bramati, G Gigli, & D Sanvitto, Phys. Rev. Lett., **109**, 266407 (2012).
[19] R Cerna, Y Leger, T K Paraiso, M Wouters, F Morier-Genoud, M T Portella-Oberli, & B Deveaud, Nature Comm., **4**, 2008 (2013).
[20] A A High, A T Hammack, J R Leonard, Sen Yang, L V Butov, T Ostatnicky, M Vladimirova, A V Kavokin, T C H Liew, K L Campman, & A C Gossard, Phys. Rev. Lett., **110**, 246403 (2013).
[21] G Grosso, J Graves, A T Hammack, A A High, L V Butov, M Hanson, & A C Gossard, Nature Photon., **3**, 577 (2009).
[22] P Andreakou, S V Poltavtsev, J R Leonard, E V Calman, M Remeika, Y Y Kuznetsova, L V Butov, J Wilkes, M Hanson, & A C Gossard, Appl. Phys. Lett., **104**, 091101 (2014).
[23] B Seradjeh, J E Moore, & M Franz, Phys. Rev. Lett. **103**, 066402 (2009).
[24] N Hao, P Zhang, J Li, Z Wang, W Zhang, & Y Wang, Phys. Rev. B **82**, 195324 (2010).
[25] J C Budich, B Trauzettel, & P Michetti, Phys. Rev. Lett. **112**, 146405 (2014).
[26] D I Pikulin & T Hyart, Phys. Rev. Lett. **112**, 176403 (2014).
[27] G Panzarini, L C Andreani, A Armitage, D Baxter, M S Skolnick, V N Astratov, J S Roberts, A V Kavokin, M R Vladimirova, & M A Kaliteevski, Phys. Rev. B, **59**, 5082 (1999).
[28] M Z Maialle, E A de Andradae Silva, & L J Sham, Phys. Rev. B, **47**, 15776 (1993).
[29] M Matuszewski, T C H Liew, Y G Rubo, & A V Kavokin, Phys. Rev. B, **86**, 115321 (2012).
[30] M M de Lima, M van der Poel, P V Santos, & J M Hvam, Phys. Rev. Lett., **97**, 045501 (2006).
[31] J Rudolph, R Hey, & P V Santos, Phys. Rev. Lett., **99**, 047602 (2007).
[32] E A Cerda-Méndez, D N Krizhanovskii, M Wouters, R Bradley, K Biermann, K Guda, R Hey, P V Santos, D Sarkar, & M S Skolnick, Phys. Rev. Lett., **105**, 116402 (2010).
[33] E A Cerda-Méndez, D Sarkar, D N Krizhanovskii, S S Gavrilov, K Biermann, M S Skolnick, & P V Santos, Phys. Rev. Lett., **111**, 146401 (2013).
[34] N Y Kim, K Kusudo, A Loffler, S Hofling, A Forchel, & Y Yamamoto, New J. Phys., **15**, 035032 (2013).
[35] T Jacqmin, I Carusotto, I Sagnes, M Abbarchi, D D Solnyshkov, G Malpuech, E Galopin, A Lemaitre, J Bloch, & A Amo, arXiv: 1310.8105 (2013).
[36] I Shelykh, A V Kavokin, Y G Rubo, T C H Liew, and G Malpuech, Semicond. Sci. Technol. **25**, 013001 (2010).
[37] F Manni, et al., Phys. Rev. B, **83**, 241307(R) (2011).
[38] We assume that the coupling to other (e.g., dark) excitons can be neglected (see, e.g., Ref. [36]).
[39] M. Plihal & A. A. Maradudin, Phys. Rev. B, **44**, 8565 (1991).
[40] M. Polini, F. Guinea, M. Lewenstein, H.C. Manoharan, & V. Pellegrini, Nat. Nanotechnol. **8**, 625 (2013).
[41] P Walker, et al., Phys. Rev. Lett., **106**, 257401 (2011).
[42] M D Martin, G Aichmayr, L Viña, & R André, Phys. Rev. Lett., **89**, 077402 (2002).
[43] A V Kavokin, et al., Phys. Rev. B, **88**, 195309 (2013).
[44] A A High, J R Leonard, A T Hammack, M M Fogler, L V Butov, A V Kavokin, K L Campman, & A C Gossard, Nature, **483**, 584 (2012).
[45] O Kyriienko, E B Magnusson, & I A Shelykh, Phys. Rev. B, **86** 115324 (2012).
[46] M M Glazov, T Amand, X Marie, D Lagarde, L Bouet, and B Urbaszek, Phys. Rev. B **89**, 201302(R) (2014).
[47] C R Zhu, K Zhang, M Glazov, B Urbaszek, T Amand, Z W Ji, B L Liu, and X Marie, Phys. Rev. B **90**, 161302(R) (2014).
[48] A V Nalitov, D D Solnyshkov, & G Malpuech, Phys. Rev. Lett. **114**, 116401 (2015).